COMMUNICATION

FUNCTIONAL RECONSTITUTION AND STRUCTURAL CHARACTERIZATION OF THE PLANT HORMONE RECEPTOR ETR1 IN LIPID NANODISCS

Received 00th January 20xx, Accepted 00th January 20xx

DOI: 10.1039/x0xx00000x

Moritz Lemke ^a, Jens Reiners ^b, Sander H.J. Smits ^{b,c}, Nils Lakomek ^d, Georg Groth ^{a,*}

The plant hormone receptor ETR1 regulates many highly relevant agronomic processes. Today significant functional and structural questions remain unanswered for its multi-pass transmembrane sensor domain able to bind and respond to the gaseous plant hormone ethylene at femtomolar concentrations. A significant reason for this is the lack of structural data on full-length ETR1 in a lipid environment. Herein, we present the functional reconstitution of recombinant full-length ETR1 purified and solubilized from a bacterial host into lipid nanodiscs allowing to study the purified plant receptor for the first time in a detergent-free membrane-like environment.

The gaseous plant hormone ethylene is associated with a wide range of developmental processes in plants such as growth, fruit ripening, abscission and senescence¹. In all these processes binding of the ethylene molecule to a membrane receptor marks the initial step in the signal transduction pathway. Genetic studies have identified that the plant Arabidopsis thaliana has five receptor isoforms (named ETR1, ERS1, ETR2, ERS2, and EIN4) for ethylene perception²⁻⁴. These ER-bound receptors, which are active only in their dimeric or higher oligomeric state, all share a similar domain architecture akin to bacterial two-component histidine kinases. An N-terminal transmembrane domain (TMD) formed by three helices, which constitute the intramembrane ethylene binding site, is followed by a GAF (cGMP-specific phosphodiesterases, adenylyl cyclases, and FhIA) domain and a catalytic transmitter domain. In three of the five receptor isoforms (ETR1, ETR2 and EIN4) the catalytic domain is further followed by a C-terminal receiver domain. In recent years, biophysical techniques for structure determination like X-ray crystallography, small-angle X-ray scattering (SAXS), nuclear magnetic resonance spectroscopy (NMR) and cryogenic electron microscopy (cryo-EM) have greatly developed. Therewith high-resolution structures of individual domains of the soluble extra-membranous part of ethylene receptors ETR1 and ERS1 have been obtained5. Besides, a computational ab-initio structural model of the transmembrane sensor domain of ETR1 has been predicted⁶ and experimentally refined by EPR spectroscopy.7 Still, the structure of the full receptor, as well as structural reorganisation and dynamics of the receptor in response to the ethylene signalling molecule remain elusive. In the past, much of the work that fostered our understanding on structure and downstream signalling interactions of the ethylene receptor family was obtained with detergent-solubilised protein.8-10 In spite of their favourable role as solubilising agents for functional and structural investigation of membrane proteins and their ability to mimic lipid environments, detergents also have their drawbacks. First, they differentiate vastly from natural cell membranes and thus do not provide an ideal native-like environment for membrane proteins (MP) which was shown vital for various MPs in order to preserve their native structure and functionality.11 Further, detergents can compromise MP stability by unfavourable interactions with their extramembranous soluble domains.¹² For these reasons, alternative solubilization and stabilization approaches have been developed over the last few decades. Amongst these lipid nanodiscs (NDs) – discoidal lipid bilayer enframed and stabilized by amphipathic membrane scaffold proteins (MSP) - take on a primary role. Their use has substantially fostered MP research and paved the way for high-resolution structural and functional studies of several bacterial and mammalian MPs.¹³⁻¹⁵ Inspired by this success, we were determined to further exploit NDs also for structural and functional analysis of plant MPs as so far only the single-pass transmembrane plant receptor-like kinase

^{*}Corresponding author. Email: georg.groth@hhu.de

^a Institute of Biochemical Plant Physiology, Heinrich Heine University Düsseldorf, Universitätsstr.1, 40225 Düsseldorf, Germany.

b. Center for Structural Studies, Heinrich Heine University Düsseldorf, Universitätsstr.1, 40225 Düsseldorf, Germany.

Institute of Biochemistry, Heinrich Heine University Düsseldorf, Universitätsstr.1, 40225 Düsseldorf, Germany.

d. Institute of Physical Biology (IPB), Heinrich Heine University Düsseldorf, Universitätsstr.1, 40225 Düsseldorf, Germany

COMMUNICATION ChemComm

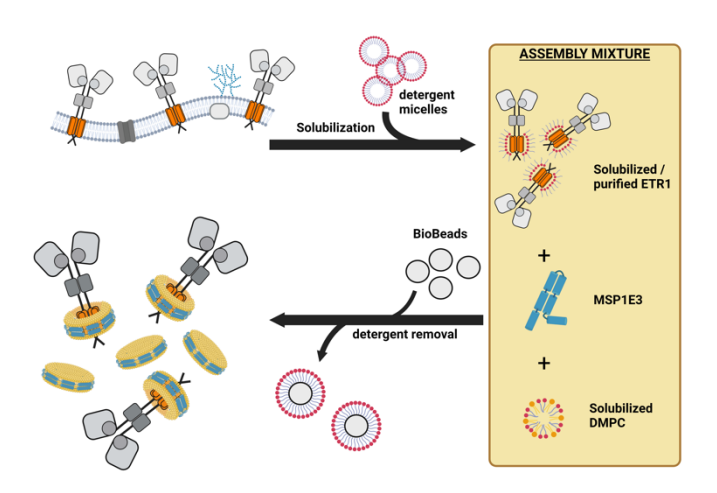


Fig. 1 Schematic overview of the assembly procedure of lipid nanodiscs. Heterologous expressed *Arabidopsis* ETR1 in *E. coli* membranes (upper left) is solubilized with detergent. The solubilized and purified receptors are mixed with MSP1E3 scaffold proteins and detergent-solubilized DMPC lipids. After incubation, detergent is removed from the assembly mixture by the addition of BioBead SM-2 resin (Bio-Rad Laboratories, Inc., Hercules, United States). The product of the self-assembling process is a composite of ETR1-loaded and empty nanodiscs.

FERONIA has been successfully reconstituted in nanodiscs albeit at low concentration in a cell-free expression system. ¹⁶ Here, we demonstrate the first reconstitution of the multi-pass transmembrane plant receptor AtETR1 in its functional dimerized state in lipid nanodiscs at high concentration. We applied size exclusion chromatography (SEC) and small-angle X-ray scattering (SAXS) to characterize size and shape of the reconstituted NDs and used liquid NMR spectroscopy to address dynamics and folding state of the incorporated ETR1 receptor. In addition to our structural studies, we analysed nucleotide binding to the reconstituted nanodiscs to further substantiate functional integration and folding of the ETR1 receptor kinase in the model phospholipid bilayer system.

In order to accomplish functional reconstitution of the first plant multi-span transmembrane receptor, AtETR1 fused to an N-terminal 10xHis-Tag was heterologously expressed in *E. coli* C43 cells in fed-batch culture. The ETR1 containing *E. coli* membranes were isolated, solubilized with detergent (n-tetradecyl-phosphocholine, Fos-Choline-14) and purified via immobilized metal affinity chromatography (IMAC). Here Fos-Choline-14 (critical micelle concentration, cmc 0.013 mM) presents a good compromise between its solubilization abilities (the lower the cmc, the better the solubilization), and ETR1 reconstitution into lipid ND in its functional state (the higher the cmc, the better for ND reconstitution).

For reconstitution of isolated receptors into nanodiscs, AtETR1 was mixed with scaffold protein MSP1E3 and 1,2-dimyristoyl-sn-glycero-3-phosphocholine (DMPC; Avanti Polar Lipids, Inc., Alabaster, United States) at a molar ratio of 2:2:240 which was determined in preceding small-scale screening experiments, where protein:lipid ratios were systematically varied based on previously reported nanodisc assembly strategies¹⁴. At the above-mentioned stoichiometry an optimal proportion of

loaded versus empty discs were obtained while maintaining a generally low amount of excessive "free" MSP, lipids and aggregates. Empty discs with an adapted molar ratio of 2:300 (MSP:DMPC) were assembled as control. The self-assembling process of the ETR1 MSP1E3 lipid nanodiscs was initiated by the addition of detergent-binding Bio-bead SM-2 resin (Bio-Rad Laboratories, Inc., Hercules, United States). Fig. 1 schematically summarizes the overall reconstitution protocol. The assembled nanodiscs were further processed by SEC in order to discriminate reconstituted from empty NDs (Fig. 2A). Moreover, elution volumes were correlated to the apparent Mw of the nanodiscs based on previous calibration with a set of welldefined protein standards. Peak fractions were then analyzed by SDS-PAGE (Fig. 2 B) which indicate the presence of ETR1 and MSP1E3 in the same fractions as expected with successful ND assembly. To substantiate ETR1 assembly in ND, proteins were labelled prior assembly with different fluorescent dyes (ETR1 with Alexa™488 and MSP1E3 with Alexa™555 (Thermo Fischer Scientific, Waltham, United States)). The related SEC profile in Fig. 2 A is characterized by two elution peaks. Taking into account the different labelling efficiencies of 0.7 dyes/ETR1 and 1.7 dyes/MSP1E3, detected fluorescence intensities in first elution peak at ~14,8 mL indicate similar amounts of ETR1 and MSP in these fractions. Based on the fact that 2 MSP molecules

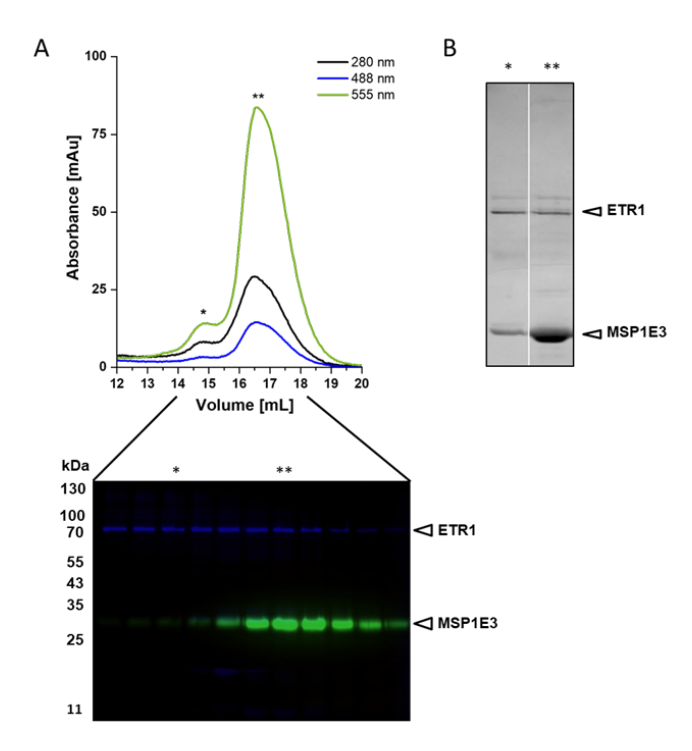


Fig. 2 (A) Size exclusion chromatography of Alexa-labeled ETR1-NDs. Prior reconstitution ETR1 was selectively labeled with Alexa™488 and MSP1E3 with Alexa™555. Absorbance was measured in mAu at 280 nm (black line), 488 nm (blue line) and 555 nm (green line). Elution peak 1 (asterisk) and elution peak 2 (two asterisks) are shown. Eluted fractions between 14 mL and 18 mL were collected in volumes of 0.4 mL and further analyzed by SDS-PAGE (below). Protein bands were detected by in-gel fluorescence imaging (Amersham Imager 680). (B) SDS-PAGE of pooled fractions from both elution peaks stained by Coomassie. Band intensity was quantified by densitometry.

ChemComm COMMUNICATION

are required to stabilize the ND lipid bilayer this strongly supports the conclusion that ETR1 assembled into NDs as a dimer. The later peak at ~17,0 mL contains - based on more intense signals at 555 nm - substantially higher amounts of MSP1E3 reflecting a large amount of empty NDs in these fractions. Analysis of SEC fractions by SDS-PAGE and in-gel fluorescence imaging or colloidal Coomassie staining substantiate these conclusions. Quantitative analyses of band intensities on Coomassie-stained SDS-PAGE gels reveal an ETR1:MSP ratio of 1:1.4 in the leading peak in agreement with previous argumentations that ETR1 is assembled into the NDs as a dimer. Furthermore, calculations indicate that about 70% of NDs in the first peak are occupied by ETR1 (see Fig. S5). It is worth to mention that we used Ni-NTA-based affinity chromatography in an alternative approach to enrich the reconstituted ETR1-NDs via the N-terminal His-tag of the receptor and remove empty discs. Naturally, MSP proteins whose His-tag has been cleaved off before the reconstitution process were applied in this approach. Unfortunately, we were not able to obtain sufficient binding of ETR1-NDs in these experiments. We suspect that due to the extended DMPC headgroup's diametric dimensions of Ø=8,5 Å as to Ø=3,0 Å of Fos-Choline-14 the N-terminal His-Tag of embedded ETR1 remains masked to the column's matrix.

To obtain a first insight into the molecular structure of the reconstituted plant receptor, we collected SAXS data of ETR1-NDs and empty nanodiscs on beamline BM29 at the ESRF Grenoble. ^{17, 18} With size exclusion coupled small-angle X-ray scattering (SEC-SAXS), we were able to remove potential aggregates prior to measure scattering data on ETR1-ND and empty NDs. We averaged the frames from the related protein peaks and subtracted them with the corresponding buffer frames. The corresponding p(r) functions showed a typical

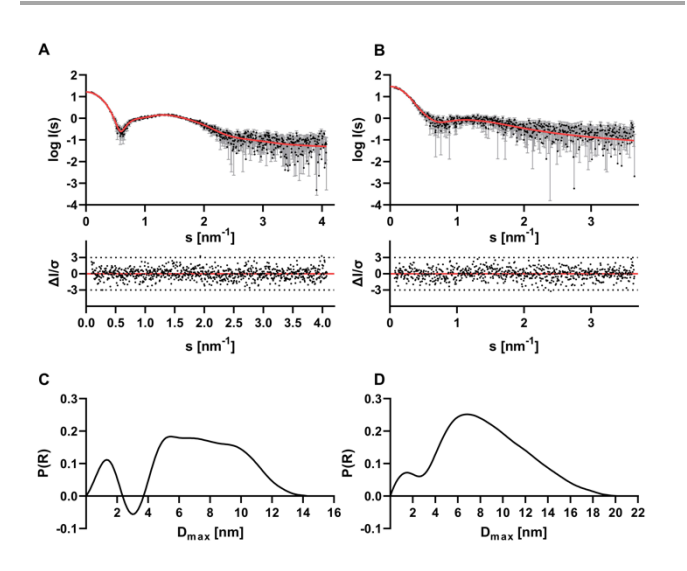


Fig. 3. Small-angle X-ray scattering data. (A) Scattering data of empty MSP1E3 nanodiscs. Experimental data are shown in black dots, with grey error bars. The GNOM fit is shown as red line. Below the residual plot of the data is shown. (B) Scattering data of ETR1-NDs. (C) The pair-distance distribution function p(r) provides a D_{max} value of 14.29 nm for empty nanodiscs and (D) a D_{max} value of 20.31 nm for ETR1-NDs.

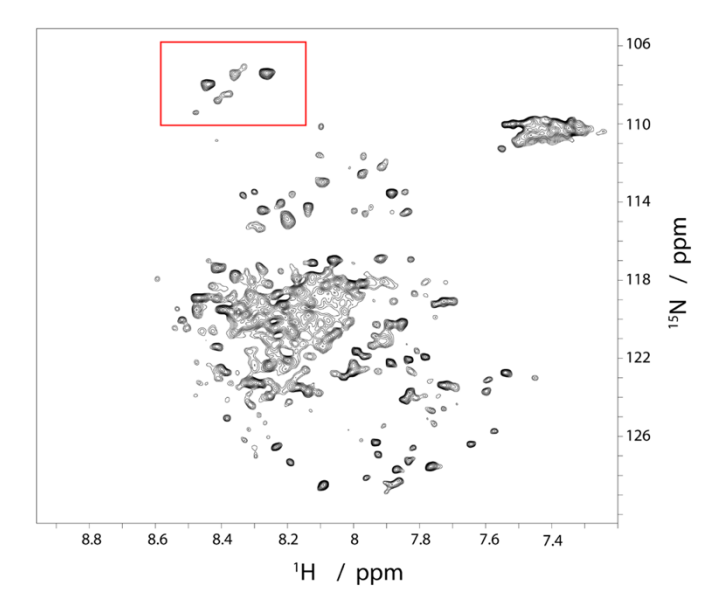


Fig. 4 Two-dimensional 1H-15N NMR correlation spectrum (HMQC-type) of 120 μ M 15N ETR1 embedded in DMPC nanodiscs and dissolved in sodium phosphate pH 6.5 buffer containing 200 mM NaCl, recorded at 10°C on a Bruker 900 MHz spectrometer. The red box in the spectrum indicates the resonances associated to Glycine residues.

distribution for the empty NDs with a determined D_{max} value of 14.29 nm, which agrees well to the theoretical dimensions of 12.9 nm for MSP1E3-NDs. For ETR1-NDs the corresponding p(r) functions indicated an extended molecule with a D_{max} value of 20.31 nm. This distribution fits the overall cylindrical shape expected for ETR1-MSP1E3-NDs based on predictions of the ETR1 dimer by AlphaFold2¹⁹ and MSP1E3-ND models²⁰.

The obtained ETR1-NDs were further assessed by NMR. A twodimensional 1H-15N NMR correlation spectrum of 15N ETR1 is shown in Fig. 4. The NMR spectrum indicates that ETR1 is wellstructured in the DMPC lipid nanodiscs. The 1H chemical shift dispersion between 7.4 and 8.6 ppm indicates α -helical structure or residues located in loop regions, respectively. Considering the high molecular weight of about 450 kDa of the ETR1 dimer in DMPC lipid nanodiscs, as revealed by size exclusion chromatography, only the most dynamic regions of ETR1 are visible to solution NMR. Because the overall weight limitation for solution NMR is about 200 kDa for the backbone of a rigid globular protein, only resonances of the most dynamic residues within the sequence remain visible in the solution 1H-15N NMR spectrum. Glycine residues resonate in a very characteristic region in an NMR spectrum, encircled here by a red box (see Fig. 4). Two intense Gly resonance signals are observable, presumably located in a highly dynamic loop region, and another five less intense Gly resonances, associated to still dynamic residues, but less dynamic than the previous two. Therefore, about seven Gly resonances out of a total of 36 Gly residues are visible in the NMR spectrum (see ETR1 amino acid sequence in SI Fig. S1). No β-strand secondary structure is visible, which would lead to a wider spectral 1H dispersion between 7 and 10 ppm. This excludes ETR1 domains with β sheet structure, such as the GAF region (region 158-307) for COMMUNICATION ChemComm

being part of the dynamic visible region. Also, the N-terminal transmembrane helices, embedded in the lipid nanodiscs are unlikely to be visible to NMR. Thus, the visible Gly resonance likely belong to residues located in the C-terminal second half of the protein (> residue 300). Previously, we had shown by circular dichroism (CD) spectroscopy that also ETR1 reconstituted into Fos-Choline-14 is well-structured.8 Here we show the first structural characterization of the ETR1 / lipid ND complex by two-dimensional NMR spectroscopy, with residue-specific resolution.

All members of the ethylene receptor family represent membrane-bound protein kinases containing a functional nucleotide binding site. To validate that ETR1 in the reconstituted NDs is in a functional state we applied the nucleotide-analog 3′-O-(N-Methylanthraniloyl) adenosine 5′ -triphosphate (MANT-ATP) as a fluorescent probe to measure and demonstrate functional nucleotide binding with the reconstituted receptor kinase. Upon addition of ETR1, a clear increase in fluorescence and blue shift in the emission maxima is observed indicative of productive nucleotide binding to the receptor kinase. Such binding was only observed in the presence of the physiological co-factor for nucleotide binding magnesium. As expected, no nucleotide binding was observed with empty NDs (see Fig. S3). In conclusion, the data presented herein confirm that we successfully reconstituted the fulllength plant ethylene receptor ETR1 from A. thaliana into lipid nanodiscs. We confirmed the reconstitution by SEC, SDS-PAGE, SEC-SAXS and solution NMR analyses. ETR1 incorporated in lipid bilayer discs maintains its native dimerized confirmation as shown by SEC and SDS-PAGE. Scattering data from SAXS experiments allowed for novel insights into the molecular structure of ETR1-NDs and well met the theoretical dimensions of empty and ETR1-incorporated nanodiscs. The chemical shift signals obtained from solution NMR indicate that the reconstituted ETR1 preserves its native folding state in the ND membrane mimetic environment. Based on these findings and specific nucleotide binding observed with the reconstituted receptor we propose that ETR1 has been reconstituted in a fully functional state. The ETR1-NDs presented in this work now build an ideal platform for further studies with biophysical techniques like solid-state magic angle spinning NMR and high-resolution cryo-EM to finally shed more light on the so far elusive structural domains and dynamics of ethylene signaling receptors.

This work was funded by the Deutsche Forschungsgemeinschaft (DFG, German Research Foundation) project no. 267205415 / CRC 1208 grant to G.G. (TP B06). The Center for Structural Studies (CSS) acknowledges funding by DFG Grant number 417919780, INST 208/761-1 FUGG) and N.L. acknowledges the DFG for funding through the Heisenberg Program (DFG grant number 433700474). We acknowledge the European Synchrotron Radiation Facility for the provision of synchrotron radiation facilities and thank Anton Popov for assistance at the beamline. We further acknowledge access to the Jülich Düsseldorf Biomolecular NMR Center, jointly run by Forschungszentrum Jülich and HHU.

Conflicts of interest

The authors declare no conflict of interest.

Notes and references

- F. B. Abeles, Morgan, P.W. and Saltveit, M.E., Ethylene in Plant Biology, Academic Press, San Diego, 1992.
- 2. B. M. Binder, J Biol Chem, 2020, 295, 7710-7725.
- 3. C. Chang, S. F. Kwok, A. B. Bleecker and E. M. Meyerowitz, *Science*, 1993, **262**, 539-544.
- 4. J. Hua, C. Chang, Q. Sun and E. M. Meyerowitz, *Science*, 1995, **269**, 1712-1714.
- H. Mayerhofer, S. Panneerselvam, H. Kaljunen, A. Tuukkanen, H. D. Mertens and J. Mueller-Dieckmann, *J Biol Chem*, 2015, 290, 2644-2658.
- S. Schott-Verdugo, L. Muller, E. Classen, H. Gohlke and G. Groth, Sci Rep, 2019, 9, 8869.
- A. Kugele, B. Uzun, L. Muller, S. Schott-Verdugo, H. Gohlke,
 G. Groth and M. Drescher, RSC Adv, 2022, 12, 7352-7356.
- 8. E. Classen and G. Groth, *Mol Membr Biol*, 2012, **29**, 26-35.
- J. Voet-van-Vormizeele and G. Groth, Mol Plant, 2008, 1, 380-387.
- Z. Gao, C. K. Wen, B. M. Binder, Y. F. Chen, J. Chang, Y. H. Chiang, R. J. Kerris, 3rd, C. Chang and G. E. Schaller, *J Biol Chem*, 2008, 283, 23801-23810.
- 11. Y. Guo, Crystals (Basel), 2020, 10.
- Z. Yang, C. Wang, Q. Zhou, J. An, E. Hildebrandt, L. A. Aleksandrov, J. C. Kappes, L. J. DeLucas, J. R. Riordan, I. L. Urbatsch, J. F. Hunt and C. G. Brouillette, *Protein Sci*, 2014, 23, 769-789.
- I. G. Denisov and S. G. Sligar, Nat Struct Mol Biol, 2016, 23, 481-486.
- F. Hagn, M. L. Nasr and G. Wagner, *Nat Protoc*, 2018, 13, 79-98.
- A. Viegas, T. Viennet and M. Etzkorn, *Biol Chem*, 2016, 397, 1335-1354.
- B. B. Minkoff, S. I. Makino, M. Haruta, E. T. Beebe, R. L. Wrobel, B. G. Fox and M. R. Sussman, *J Biol Chem*, 2017, 292, 5932-5942.
- 17. P. Pernot, P. Theveneau, T. Giraud, R. N. Fernandes, D. Nurizzo, D. Spruce, J. Surr, S. McSweeney, A. Round, F. Felisaz, L. Foedinger, A. Gobbo, J. Huet, C. Villard and F. Cipriani, *Journal of Physics: Conference Series*, 2010, **247**.
- P. Pernot, A. Round, R. Barrett, A. De Maria Antolinos, A. Gobbo, E. Gordon, J. Huet, J. Kieffer, M. Lentini, M. Mattenet, C. Morawe, C. Mueller-Dieckmann, S. Ohlsson, W. Schmid, J. Surr, P. Theveneau, L. Zerrad and S. McSweeney, J Synchrotron Radiat, 2013, 20, 660-664.
- J. Jumper, R. Evans, A. Pritzel, T. Green, M. Figurnov, O. Ronneberger, K. Tunyasuvunakool, R. Bates, A. Zidek, A. Potapenko, A. Bridgland, C. Meyer, S. A. A. Kohl, A. J. Ballard, A. Cowie, B. Romera-Paredes, S. Nikolov, R. Jain, J. Adler, T. Back, S. Petersen, D. Reiman, E. Clancy, M. Zielinski, M. Steinegger, M. Pacholska, T. Berghammer, S. Bodenstein, D. Silver, O. Vinyals, A. W. Senior, K. Kavukcuoglu, P. Kohli and D. Hassabis, Nature, 2021, 596, 583-589.
- Y. Qi, J. Lee, J. B. Klauda and W. Im, J Comput Chem, 2019, 40, 893-899.